Behavior of Mixed-Oxide Fuel Elements in a Tight Bundle under Duty-Cycle Conditions

T. ASAGA, S. SHIKAKURA
Power Reactor and Nuclear Fuel Development Corporation, Oarai, Japan
H. TSAI, L. A. NEIMARK
Argonne National Laboratory, Argonne, IL USA

1. INTRODUCTION

A bundle of 37 mixed-oxide fuel elements (also referred as fuel pins) was irradiated in EBR-II as part of the joint Operational Reliability Testing (ORT) program between the U.S.Department of Energy and PNC of Japan [1]. The test, designated as TOB-10, consisted of steady-state power operation superimposed with periodic ~20% overpower duty-cycle transients. In conjunction with the companion "single pin" tests conducted under comparable irradiation conditions [2], the objective of the TOB-10 test was to investigate the effects of pin bundle-duct interaction on fuel pin performance, including lifetime. The bundle porosity in the TOB-10 test was intentionally reduced to accentuate pin bundle-duct interaction. In the single-pin tests, on the other hand, each pin was irradiated inside a flow tube which eliminated thermal and mechanical interactions between the pins.

The test fuel pins in the TOB-10 test, in the single-pin test nomenclature, belonged to the conservative-to-moderate categories, and were expected to have an extended lifetime, >10,000 effective full power hours (EFPHs). By employing pins of conservative/moderate designs, the strategy of the TOB-10 test was to reach bundle closure before reaching the endurance limits of the single pins. Any accelerated cladding breaching after the bundle closure, with respect to the single pin breaching statistics, could then be evaluated in the context of pin bundle-duct interaction.

2. SPECIFICATION OF SUBASSEMBLY AND FUEL PINS

Thirty-seven mixed-oxide fuel pins, with three different designs, were used in the TOB-10 test. The key design parameters of the pins, categorized as groups A, B, C, are shown in Table 1. All of the pins had 5.84-mm O.D., 0.381-mm thick cladding, 1016-mm overall length, and 343-mm long fuel column. The principal design variables were cladding material (20% CW Type D9 and 20% CW Type 316 stainless steel), pellet density (89 and 93% TD), and diametral gap (0.069 to 0.124 mm).

Pin-to-pin spacing within the TOB-10 bundle was maintained by helical wrapping wires made of the same materials as the cladding. To reduce the bundle porosity and accelerate bundle closure, oversized wrapping wires, 1.482-mm dia., instead of the nominal wires of 1.422-mm dia., were used. The

Table 1. Key Design and Irradiation Parameters for the TOB-10 Test Pins

	Group A (20 pins)	Group B (8 pins)	Group C (9 pins)
Pellet Density (% TD)	88.9	88.6	93.4
Diametral Gap (mm)	0.069	0.124	0.084
Smear Density (% TD)	86.5	84.3	90.3
Fuel O/M	1.96	1.95	1.96
Fuel Pellet Form	Dished	Dished	Dished
Clad Material	D9	316SS	316SS
Clad Cold Work	20%	20%	20%
EOL Peak LHR (kW/m)	31.8-34.8	30.5-31.8	34.4-36.4
EOL Peak BU (a/o)	7.3-7.9	7.8-8.1	7.3-7.7
EOL Peak Fast Fluence (x 10^{22} n/cm^2)	5.0-5.5	5.4-5.6	5.1-5.3
EOL Peak Clad MW Temp (°C)	629	632	634

helical wire pitch was 305 mm (12 in.). The nominal bundle porosity in the TOB-10 subassembly was 0.25 mm (flat-to-flat), for a nominal pin-to-pin clearance of 0.041 mm. Assuming all pins strain equally, bundle closure would occur at the peak cladding strain of ~0.7%.

3. IRRADIATION TEST

The irradiation started in EBR-II Run 128. After the first steady state irradiation period, the first scheduled mild overpower transient was conducted by relocating the subassembly from the steady-state core location (outer-row) to an inner-row location. Following three days of partial power preconditioning, the reactor power was raised to the full power at a ramp of ~0.3%/s and held at the full power for 5min. The attained overpower in individual pins ranged from 19 to 26%. In this same manner, the irradiation of the TOB-10 test continued in the next four runs and similar overpower transient was conducted at the end of each run.

After 7712 EFPHs of irradiation, at ~8 a/o peak burnup, two test pins developed cladding breach and the test was terminated. At the time of termination, the steady-state linear power of the test pins ranged from 30 to 36 kW/m, with a peak mid-wall cladding temperature of ~630°C. The test pins were subjected to five mild transients of 12 to 32% overpower in individual pins, approximately evenly spaced during the steady-state irradiation. The irradiation parameters for the TOB-10 test pins are shown in Table 1.

4. BEHAVIOR OF FUEL PINS

During postirradiation examination, two breached pins, both D9-clad, were identified. None of the 316SS-clad pins, some with higher fuel smear densities, developed breach. The condition of the cladding breach is shown in Fig.1. Both cladding breaches were longitudinal cracks, initiated under the wire and at an axial location near the top of the fuel, x/l=~0.93. The appearance of the cladding breach suggested the failure mode was a gas-driven burst rupture. The significant nondestructive and destructive examination results for the TOB-10 fuel pins are presented below.

4.1 Cladding deformation

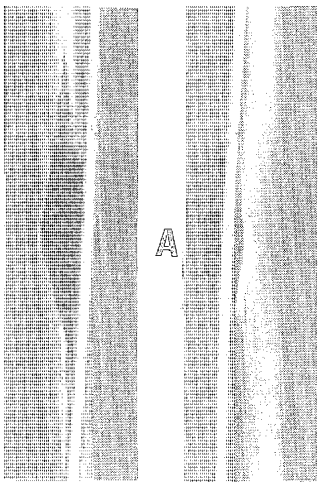

Fig.1. Two views of the cladding breach of the D9-clad pins. The bulge at "A" caused the contact with a neighboring pin.

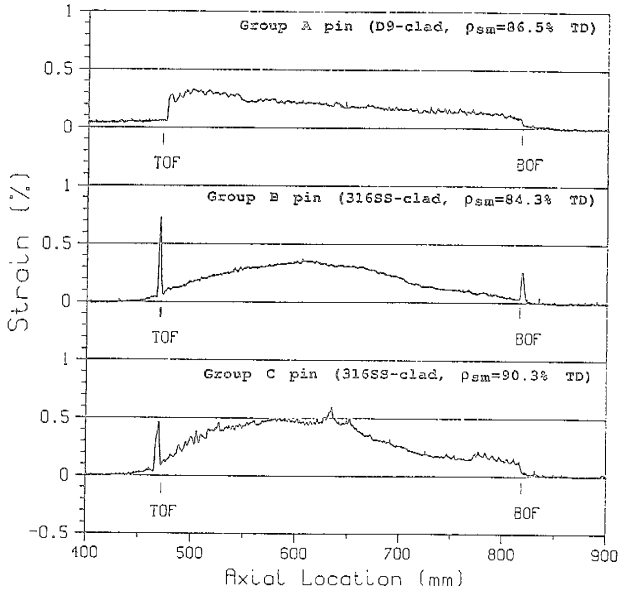

Fig.2. Cladding strain profiles of three TOB-10 test fuel pins with different designs.

The strain profiles for the TOB-10 fuel pins vary systematically with pin design, particularly, cladding material. The measured cladding strain profiles for the D9- and 316SS-clad pin groups are illustrated in Fig.2. The overall strain for the D9-clad pins was small, with a maximum of ~0.30%. At the top end of the fuel column, there was a region of increased strain. This strain plateau, ~70-100 mm long, appeared to be present in the two breached pins as well. The step change of the strain profile at the end of the fuel column indicated that the strain in the low-swelling D9 clad-pins was induced mainly by fuel/cladding mechanical interaction (FCMI).

The strain profiles of the 316SS-clad pins, on the other hand, had a generally chopped-cosine shape with the sharp strain peaks at the end of the fuel column. The maximum strain in the fuel column was also small, ~0.4-0.5%, occurring x/l=~0.6. The chopped-cosine strain profiles in the fuel column region in the 316SS-clad pins suggested that a significant portion of the overall strain in the fuel column region was due to irradiation-induced swelling of the 316SS cladding material.

The results on cladding strain in the TOB-10 test are summarized in Table 2. Neither the D9- nor 316SS-clad pin groups attained the nominally required cladding strain of 0.7% for bundle closure. Consequently, no substantial pin bundle-duct interaction would be expected. This was confirmed by the lack of any appreciable cladding ovality in any of the pins examined.

The strain profiles of the D9- and 316SS-clad pins from the sibling single-pin tests display essentially the same strain profile features. The magnitude of the strains in the single pins, shown in Table 2, are somewhat greater due to the higher burnup and fluence of the sibling pins.

Table 2. Comparison of measured cladding strain in the TOB-10 test and the single pin tests

Pin Type	Test ID	Test Design	Peak Burnup (at%)	Peak Fast Fluence 10^{22}n/cm^2	Peak Cladding Strain (%)	Peak Cladding Strain X/L location
D9, group A	TOB-10	Bundle, OP	7.6	5.3	0.3	0.9
	TOP-4A	Pin, SS	8.8	6.1	0.6	0.9
	TOP-4B	Pin, OP	9.7	6.4	0.7	0.9
316, group B	TOB-10	Bundle, OP	8.0	5.5	0.4	0.6
	TOP-4A	Pin, SS	8.6	5.9	0.55	0.6
	TOP-4B	Pin, OP	9.2	6.2	0.65	0.6
316, group C	TOB-10	Bundle, OP	7.5	5.2	0.5	0.65
	TOP-4A	Pin, SS	9.1	6.3	0.7	0.65
	TOP-4B	Pin, OP	9.8	6.5	1.1	0.6

SS: steady-state operation
OP: steady-state plus periodic overpower transient

4.2 Distribution of volatile fission product cesium

Another feature of interest is the significant effect of volatile fission product cesium on the cladding strain. For the D9-clad pins, essentially all of the cesium fission product remained within the fuel column. There was no evidence of cesium migration beyond the fuel column and reacting with the UO_2 insulator pellets. For the 316SS-clad pins, however, migration of cesium beyond the fuel column region was evident. For group B (lower fuel smear density) pins, cesium activity peaks were found at both the upper and lower insulator pellets. For the group C (higher fuel smear density) pins, a cesium peak was present only at the top. The locations of these peaks correspond with those of strain peaks.

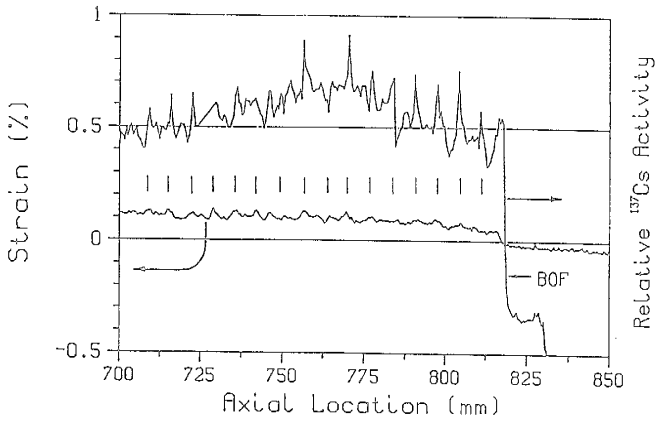

Fig.3. Correlation between the local strain peaks and accumulation of ^{137}Cs at the pellet/pellet interfaces (tick marks) in the bottom portion of the fuel column.

Within the fuel column, the cesium distribution pattern showed local variations depending on the axial location. In the cooler bottom portion of the fuel, cesium accumulated predominantly at the pellet/pellet gaps, as shown in Fig.3 for a D9-clad pin. The superimposed cladding strain profile showed that the periodic high strain peaks are associated with the cesium buildup at the pellet/pellet interface. In the upper portion of the fuel column, shown in Fig.4, there were greater cesium activities along the fuel pellet than at the pellet/pellet interfaces. Metallography and electron microprobe analyses indicated that the cesium at these upper locations had reacted extensively with the cladding but little the fuel (see below). The cesium in the cooler region may be in compounds with other fission products, such as Cs_2MoO_4. That in the hotter region may be reaction compounds with the cladding, such as cesium chromates. An electron microprobe examination is under way to identify the chemical forms for the Cs-bearing compounds in bottom regions.

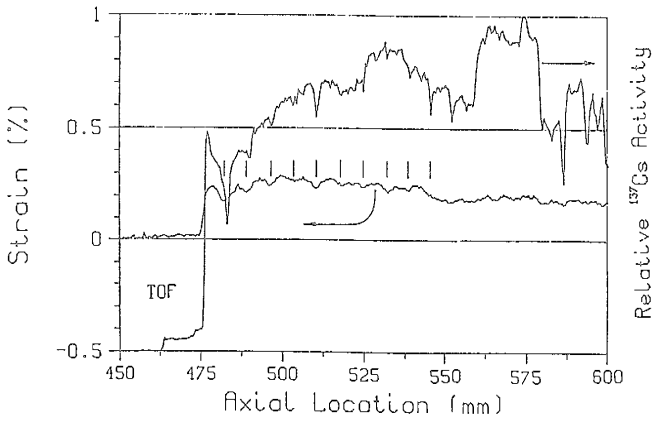

Fig.4. Correlation between the local strain minima and ^{137}Cs distribution in the top portion of the fuel column. The tick marks denote the pellet/pellet interfaces.

4.3 Fuel/cladding interaction

Metallographic examination revealed significant fuel/cladding chemical interaction (FCCI) near the top end of the fuel column in the D9-clad pins, as shown in Fig.5. There was appreciable cladding wastage due to the FCCI; the wastage was smaller at pellet/pellet interface, corresponding to the cladding strain pattern mentioned above. The maximum cladding wastage was ~80μm (~20% of the cladding thickness), somewhat greater than that observed in the D9-clad fuel pins in the single-pin tests. Penetration into the cladding was predominantly a broad-front matrix attack, which filled the fuel/cladding gap. The FCCI in the 316SS-clad pins was minor and resulted in no measurable cladding wastage.

Both cladding breach in the D9-clad pins took place near the top of the fuel column where extensive FCCI and cladding thinning occurred. Meanwhile, cladding profilometry data showed no appreciable cladding ovality in any of the pins examined. This suggested that pin bundle-duct interaction was minimal and not a principal cause of cladding breach. The principal cause of cladding breach in the TOB-10 test was apparently the significant cladding thinning resulting in an increased hoop stress in the cladding. In addition, the fission gas pressure in the central void in the fuel column could have been substantially enhanced due to FCCI-induced blockage. The burst-type rupture of the cladding in the fuel column region strongly suggested high gas pressure in the fuel column.

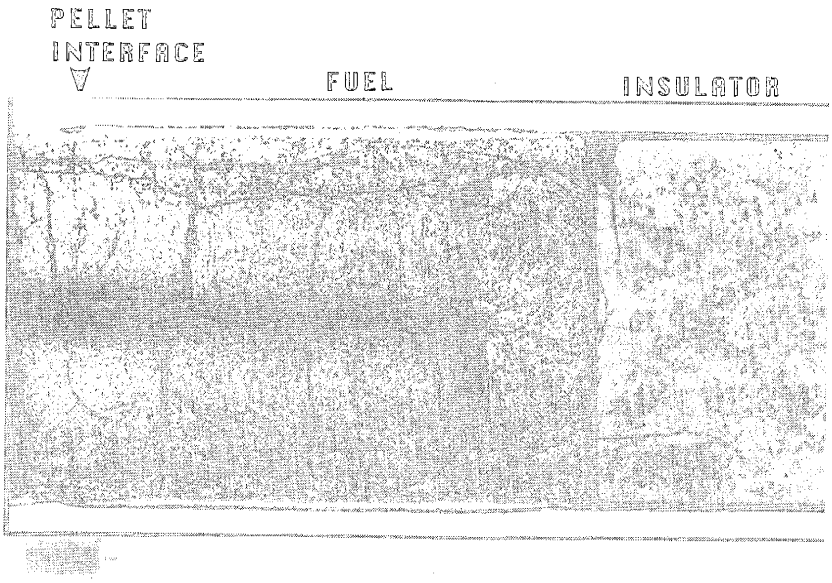

Fig.5. Fuel/cladding chemical interaction of the D9-clad pins. (at the top end of the fuel column)

5. CONCLUSIONS

(1) The irradiation behavior of the TOB-10 fuel pins was comparable with that obtained in the single pin tests. There was no significant effect that could be directly attributed to tight bundle configuration. The postirradiation examination data provided information on the axial migration of cesium and its effect on cladding strain.

(2) Severe fuel/cladding chemical interaction (FCCI), which resulted in substantial cladding thinning and probably restricted venting of fission gas from the fuel column into the pin plena, apparently caused the earlier-than-expected cladding breaches in the D9-clad pins. No such severe FCCI was noted in the 316SS-clad pins.

(3) At the time of test termination, the overall cladding strain from creep and swelling was insufficient to cause bundle closure. Consequently, there would have been minimal pin bundle-duct interaction in the subassembly. Neither of the breaches appeared to be induced by pin bundle-duct interaction.

REFERENCES

[1] Boltax, A. et al.(1985). "EBR-II Operational Transient Testing", BNES Conf. on Nuclear Fuel Performance, Stanford-upon Avon

[2] Boltax, A. et al.(1990). "Fuel Pin Behavior During Duty Cycle Testing", ANS Inter. Conf. Fast Reactor Safety Meeting, Snowbird